Quantification of regional myocardial blood flow estimation with three-dimensional dynamic rubidium-82 PET and modified spillover correction model

Chietsugu Katoh, MD, PhD,[a] Keiichiro Yoshinaga, MD, PhD, FACC,[b] Ran Klein, PhD,[c,d] Katsuhiko Kasai, BSc,[a] Yuuki Tomiyama, BSc,[a] Osamu Manabe, MD, PhD,[c] Masanao Naya, MD, PhD,[e] Mamoru Sakakibara, MD, PhD,[e] Hiroyuki Tsutsui, MD, PhD,[e] Robert A. deKemp, PhD,[d] and Nagara Tamaki, MD, PhD[c]

Purpose. **Myocardial blood flow (MBF) estimation with ^{82}Rubidium (^{82}Rb) positron emission tomography (PET) is technically difficult because of the high spillover between regions of interest, especially due to the long positron range. We sought to develop a new algorithm to reduce the spillover in image-derived blood activity curves, using non-uniform weighted least-squares fitting.**

Methods. **Fourteen volunteers underwent imaging with both 3-dimensional (3D) ^{82}Rb and ^{15}O-water PET at rest and during pharmacological stress. Whole left ventricular (LV) ^{82}Rb MBF was estimated using a one-compartment model, including a myocardium-to-blood spill-over correction to estimate the corresponding blood input function $Ca(t)^{whole}$. Regional $K1$ values were calculated using this uniform global input function, which simplifies equations and enables robust estimation of MBF. To assess the robustness of the modified algorithm, inter-operator repeatability of 3D ^{82}Rb MBF was compared with a previously established method.**

Results. **Whole LV correlation of ^{82}Rb MBF with ^{15}O-water MBF was better ($P < .01$) with the modified spillover correction method ($r = 0.92$ vs $r = 0.60$). The modified method also yielded significantly improved inter-operator repeatability of regional MBF quantification ($r = 0.89$) versus the established method ($r = 0.82$) ($P < .01$).**

Conclusion. **A uniform global input function can suppress LV spillover into the image-derived blood input function, resulting in improved precision for MBF quantification with 3D ^{82}Rb PET. (J Nucl Cardiol 2012)**

Key Words: Myocardial blood flow • positron emission tomography • ^{82}Rb • spillover correction

From the Department of Health Sciences,[a] Department of Molecular Imaging,[b] Department of Nuclear Medicine,[c] Cardiovascular Medicine,[e] Hokkaido University Graduate School of Medicine, Sapporo, Japan; and Division of Cardiology, National Cardiac PET Centre,[d] University of Ottawa Heart Institute, Ottawa, ON, Canada.

This study was supported in part by Grants from the Ministry of Education, Science and Culture (No. 19591395), Northern Advancement Center for Science & Technology (Sapporo, Japan) (#H19-C-068, H23-S2-17), and Adult Cardiovascular Foundation (Kyoto, Japan). Ran Klein was supported by the Japan Society for the Promotion of Science (JSPS) and the Natural Sciences and Engineering Research Council of Canada (NSERC) Summer Program (2008) (Tokyo, Japan and Ottawa, Ontario, Canada).

Received for publication Oct 12, 2011; final revision accepted Mar 29, 2012.

Reprint requests: Keiichiro Yoshinaga, MD, PhD, FACC, Department of Molecular Imaging, Hokkaido University Graduate School of Medicine, Kita15 Nishi7, Kita-Ku, Sapporo, Hokkaido 060-8638, Japan; *kyoshi@med.hokudai.ac.jp*.

1071-3581/$34.00

doi:10.1007/s12350-012-9558-1

Published online: 14 April 2012

INTRODUCTION

Recently, our groups and others have shown that myocardial blood flow (MBF) can be estimated using rubidium-82 (^{82}Rb) positron emission tomography (PET)[1-4] as well as PET performed using other flow tracers.[5] ^{82}Rb is a PET perfusion tracer produced from a strontium-82 (^{82}Sr)/^{82}Rb generator and is widely used for the diagnosis of coronary artery disease (CAD)[6-9] in PET centers lacking immediate access to a cyclotron. ^{82}Rb PET has good diagnostic accuracy[10-12] and also has prognostic value in patients with CAD.[13,14] The ability to quantitatively measure regional and global left ventricular (LV) MBF is one advantage of PET myocardial perfusion imaging.[15,16] Quantitative MBF can indicate the functional severity of coronary stenosis and may provide additional diagnostic information in patients with CAD.[15,17,18] It may also play an important role in the prevention of future cardiovascular events.[14,19]

Some automated or semi-automated programs, such as FlowQuant,[2,20] MunichHeart,[21] and PMOD,[22] have been developed and applied for MBF estimation with ^{82}Rb. Lortie et al[2] validated MBF quantification using a one-tissue-compartment model of ^{82}Rb kinetics, compared to ^{13}N-ammonia measurements in normal subjects and CAD patients. Our program is one of several validated automated programs for MBF quantification in humans using 3-dimensional (3D) ^{82}Rb PET. However, some variability in stress MBF has been noted in previous studies. Therefore, there is a need to further improve the analysis program for MBF quantification with ^{82}Rb especially in the 3D acquisition mode.

Current PET/computed tomography (CT) scanners offer only a 3D data-acquisition mode. The high positron energy and range, together with relatively low-count statistics from the short tracer half-life, limit the achievable spatial resolution and may impact the accuracy of ^{82}Rb MBF measurements due to spillover effects. The purpose of this study was to develop a new MBF quantification algorithm for 3D ^{82}Rb dynamic PET, and to validate it using two-dimensional (2D) ^{15}O water, which is a freely diffusible tracer with high extraction fraction at increased blood flow.[15]

MATERIALS AND METHODS

Study Subjects

Fourteen healthy men underwent 3D ^{82}Rb and 2D ^{15}O-water PET studies (mean age 31.6 ± 13.1 years). All participants had a normal resting electrocardiogram (ECG). They did not have a history of cardiovascular disease and did not take any cardiac medications. All healthy control subjects had a low pre-test likelihood of CAD) (<5%) based on their risk factors.[23]

The study was approved by the Hokkaido University Graduate School of Medicine Human Research Ethics Board. Written informed consent was obtained from all subjects.

Study Protocol

Each subject underwent rest and pharmacological stress imaging using adenosine triphosphate (ATP), with both ^{15}O-water and ^{82}Rb PET. The 2D ^{15}O-water and 3D ^{82}Rb imaging were performed on separate days in randomized order (mean interval 17.2 ± 15.4 days).

PET Acquisition Protocol

Participants were instructed to fast for 6 hours and to abstain from caffeine-containing products for 24 hours prior to PET studies.[17,24,25] Participants were positioned with the heart centered in the field of view of a whole body PET scanner (ECAT HR+, Siemens/CTI Knoxville, TN), which is capable of both 2D- and 3D-mode data acquisition.

^{15}O-Water Imaging

After a 6-minute transmission scan for attenuation correction, participants inhaled 2,000 megabecquerels (MBq) of ^{15}O-carbon-monoxide (CO) (0.14% CO mixed with room air) for 1 minute and were then imaged over 5 minutes to obtain a blood volume image.[17,26] After decay of ^{15}O radioactivity, 1,500 MBq of ^{15}O-water was administered intravenously at a slow infusion rate (2 minutes) at rest, and a 20-frame dynamic PET acquisition was initiated with varying frame durations (6 × 5 seconds, 6 × 15 seconds, 8×30 seconds) over 6 minutes.[16,25] All ^{15}O-water imaging was performed in 2D mode with septa extended.

Pharmacological stress was induced by ATP (160 μg/kg/minute × 9 minutes).[1] Three minutes after the start of the ATP, a second dynamic scan was started using the same dynamic sequence at rest. ATP was continued for a total of 9 minutes. During the entire exam, symptoms, heart rate, blood pressure, and ECG were monitored continuously.

^{82}Rb Imaging

The ^{82}Rb protocol was similar to that of ^{15}O-water except that immediately following the transmission scan, 555 MBq of ^{82}Rb (BRACCO Diagnosis, Princeton, NJ or DRAXimage, Kirkland, QC) was administered intravenously. An 8-minute 23-frame dynamic scan was initiated with increasing frame duration in 3D mode with septa retracted (18 × 10 seconds, 5 × 60 seconds).[1,14,27]

Pharmacological stress was induced by ATP (160 μg/kg/minute × 9 minutes) 10 minutes after the rest image acquisition.[1]

Quantification of MBF

Images were reconstructed using the vendor-supplied filtered back-projection software (ECAT v7.2). We used a 10-mm Hann window of the ramp filter for 2D ^{15}O-water images, and a 12-mm Hann window of the ramp filter for 3D ^{82}Rb images, respectively.[2] Each frame consisted of 63 transaxial slices each having 128 × 128 voxels with dimensions 3.4 × 3.4 × 2.4 mm. MBF quantification was performed using a software program developed in-house.[28] Regions of interest (ROIs) for the LV cavity blood pool and the LV myocardium were defined semi-automatically. The LV wall was divided into 16 segments.[16,27] The ROIs were sampled in all timeframes to derive LV blood and myocardium time-activity curves. The program then performed MBF quantification using a one-tissue-compartment tracer kinetic model.[27,28] The MBF quantification processes differed for ^{15}O-water and ^{82}Rb as described below.

^{15}O-Water Model

All frames of the water image were summed, and the blood volume image of ^{15}O-CO was then subtracted to generate a myocardial uptake image. The uptake image was used to reorient the original image to semi-automatically create short-axis slices and to automatically create the myocardial ROIs. The blood volume image was similarly reoriented and then automatically segmented to define a blood pool ROI with integral intensity equal to 85% of maximum pixel intensity. The ROIs were applied to the entire dynamic image to generate LV blood and regional myocardium time-activity curves (TACs), LV(t), and R(t), respectively. The MBF was estimated as described in the ''Appendix.''

^{82}Rb Models

Established method. With ^{82}Rb, a myocardial uptake image was generated by summing the last 5-8 minutes of the dynamic image sequence. A blood volume image was created by summing the first 2 minutes of the image sequence.[2] The images were reoriented and segmented semi-automatically to generate LV blood and myocardial TACs using the dynamic data from 0 to 8 minutes.[28]

The MBF estimation is described in the ''Appendix.''

Wavelet-based noise reduction method. A wavelet-based noise-reduction protocol was performed to eliminate noise in the measured TAC in the myocardial ROI R(t) and in the left ventricular ROI LV(t).[4] Two-compartment model analysis was also applied and MBF was estimated based on Lin's approach.[4]

Modified or dual-spillover method. For robust estimation of regional K1 and MBF, our method calculates the K1 value using a global uniform input function $Ca^{whole}(t)$, which is estimated from a whole myocardial ROI, W(t) (Figure 1). Fitting Eqs. 1, 3, and 4 yielded $K1$, $k2$, perfusable tissue fraction (PTF), and VA for the whole-myocardial ROI data, as well as the corresponding input function $Ca^{whole}(t)$. The MBF was estimated using the global uniform input function $Ca^{whole}(t)$ as described in the ''Appendix.''

Thus, the established and the modified methods differed in two aspects. (1) The modified method first estimated a pure spillover-corrected blood time-activity curve and then used it for calculating flow in all LV regions, while the established method spillover-corrected the blood input function for each myocardial region independently. (2) The established method used uniform timeframe weighting while the modified method weighed each frame by the pure spillover-corrected blood

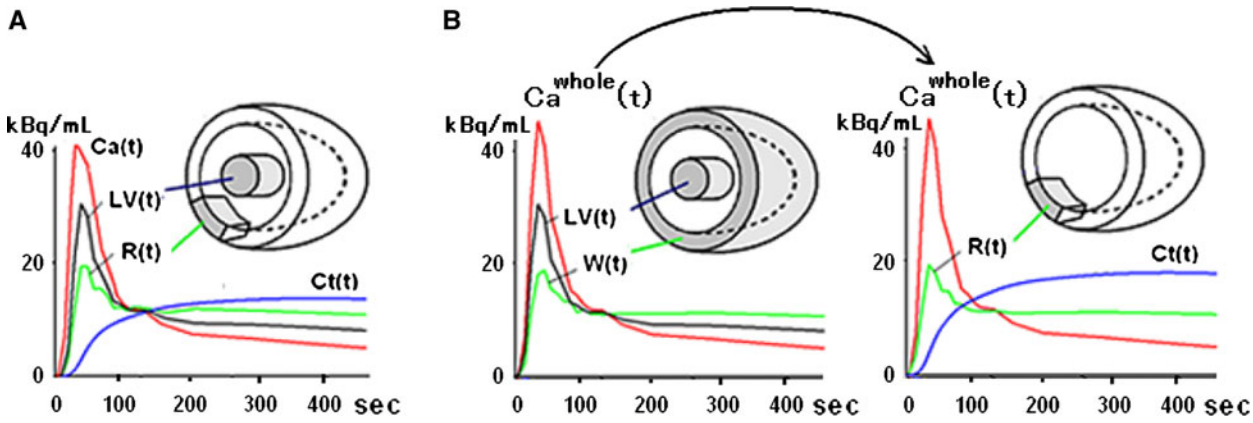

Figure 1. Scheme of the algorithm and sample data curves of the established method (**A**) and our modified method (**B**). **A** R(t) and LV(t) correspond to measured time-activity curves in a regional myocardial ROI and in the left ventricle, respectively. An input function Ca(t), tissue time-activity curve Ct(t), and regional MBF are derived from R(t) and LV(t). Different input function Ca(t) is calculated for estimation of each regional $K1$ value. **B** W(t) corresponds to a measured time-activity curve in the whole myocardial ROI. A uniform input function $Ca^{whole}(t)$ is derived from W(t) and LV(t). Then each regional MBF is estimated using this input function $Ca^{whole}(t)$ and R(t). The same input function $Ca^{whole}(t)$ is applied for estimation of each regional **K**1 value.

activity. The same LV blood and myocardial ROIs, and therefore TACs, were used for processing with both the established and the modified methods.

The estimated MBF values from the established uniform and the modified weighted methods were compared against MBF values estimated from the corresponding ^{15}O-water images.

Inter-operator Repeatability of ^{82}Rb MBF

Each 3D ^{82}Rb scan was processed by two operators using both established and modified methods. The regional MBF values obtained by the different operators were compared to assess inter-operator repeatability. The repeated studies were performed independently by two nuclear physicians, one novice and one expert. The novice user had never used the program of MBF quantification with 3D ^{82}Rb data. The expert user was the developer of this program.

Simulation Study

We performed a simulation study to evaluate the sensitivity of MBF to measurement errors in the parameter PTF, the tissue fraction in the LV myocardium ROI, using ^{15}O-water and both the established and the modified ^{82}Rb methods.

The mean myocardial and LV TACs were generated using data for the 20 subjects from 3D ^{82}Rb PET studies. The percentage error in MBF was calculated as a function of the percentage error of the parameter PTF. The percentage error of PTF was modified from -10% to $+10\%$ and the % error in MBF versus % error in PTF was plotted for each MBF quantification method.

Subjects with Known or Suspected CAD

To demonstrate the clinical utility of the global input function model, 12 patients with known or suspected CAD were recruited. At the time of these additional studies, 2D data acquisition was still standard[5] for PET MBF quantification using ^{82}Rb with an injected dose of 1480 MBq.[29] Methods for image processing and MBF estimation were the same as those described above for the healthy volunteers.

Segmentation Classification

Using quantitative coronary angiography (QCA) data, LV segments were classified into 2 groups according to whether or not they contained stenotic regions. Significant coronary stenosis was defined as $\geq$70% luminal narrowing.

Statistical Analysis

To assess the concordance between the 3D ^{82}Rb MBF and the 2D ^{15}O-water MBF, Pearson's correlation coefficients were calculated. A Bland-Altman analysis was applied to evaluate the agreement among the whole LV MBF values derived from each of these methods. To evaluate the inter-operator repeatability of the regional MBF with 3D ^{82}Rb, Pearson's correlation coefficients were calculated and the Bland-Altman analysis was applied for regional MBF. These two results were applied for the established method and the modified method. The reproducibility coefficient (RPC%) was used to evaluate agreement in results between the two operators. The differences between results using the established method and results using the modified method were compared using Fisher z-transformation. All data were presented as mean and standard deviations. A P value of $<.05$ was considered to be statistically significant in the assessment of differences in correlation coefficients and differences in variability.

RESULTS

The ATP stress was well tolerated by all participants. None of the participants had ischemic ECG changes or chest pain during ATP stress.

Hemodynamics

Heart rate and systolic blood pressure at rest were similar in ^{15}O-water and ^{82}Rb PET studies (Table 1). In both studies, rate pressure product (RPP) significantly increased during ATP stress ($P < .01$). Table 1 shows the variables of systolic blood pressure, heart rate, and RPP in the ^{15}O-water and ^{82}Rb scans in resting and hyperemic states. No significant hemodynamic change was observed during any of the dynamic acquisitions.

Table 1. Hemodynamics during ^{15}O-water and ^{82}Rb PET studies

	^{82}Rb 3D Rest	^{82}Rb 3D Stress	^{15}O-Water Rest	^{15}O-Water Stress
HR	57.6 ± 5.3	81.4 ± 11.7	57.1 ± 4.9	80.4 ± 9.4
sBP	111.1 ± 15.7	108.2 ± 14.5	105.6 ± 14.9	103.3 ± 13.5
RPP	6409 ± 1143	8812 ± 1780*	6001 ± 793	8296 ± 1362*

* $P < .01$ versus rest.
HR, Heart rate; *sBP*, systolic blood pressure; *RPP*, rate pressure product.

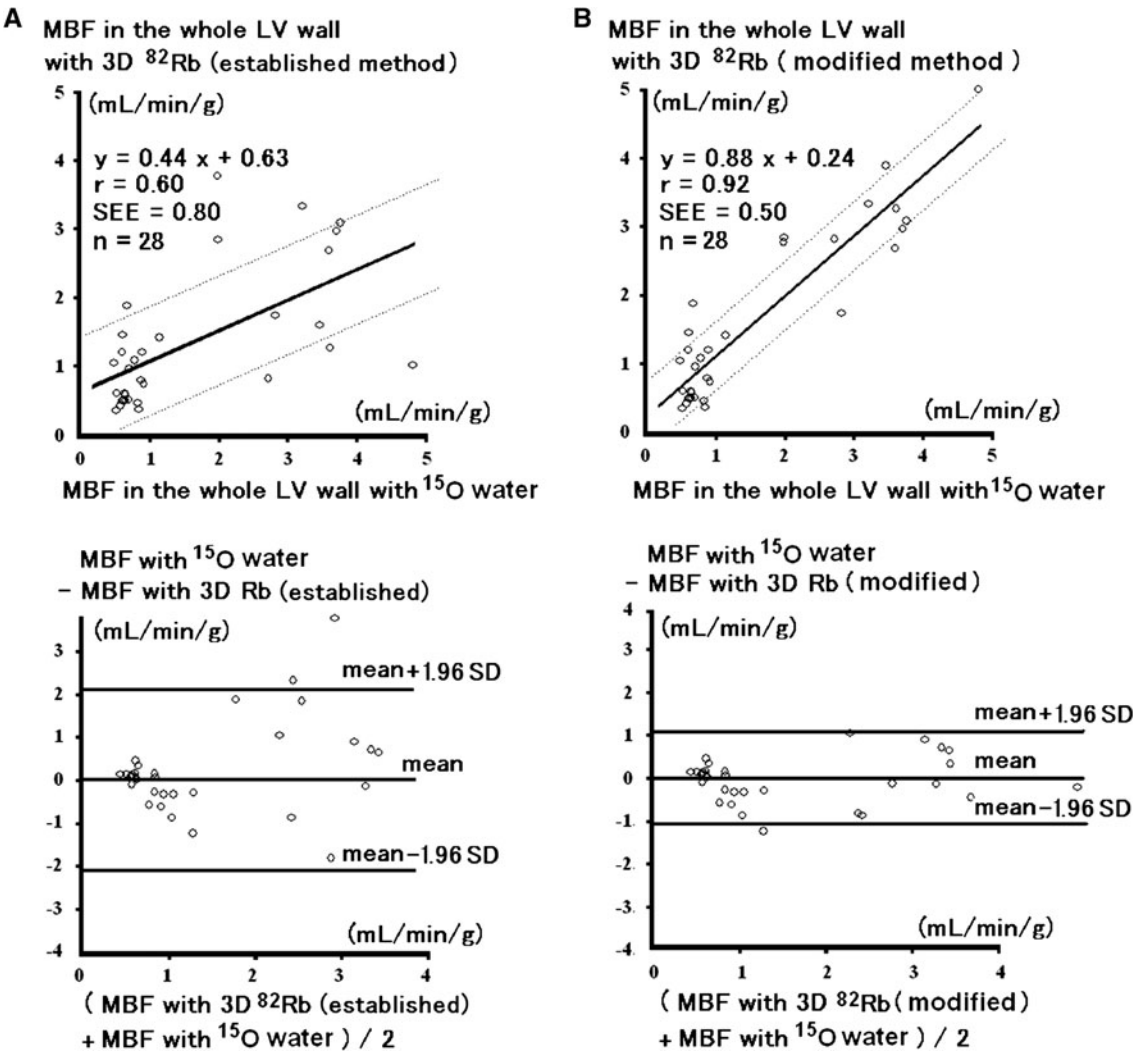

Figure 2. **A** Correlation and Bland-Altman plots of MBF in the whole LV wall with ^{15}O-water and ^{82}Rb (established method). **B** Correlation and Bland-Altman plots of MBF in the whole LV wall with ^{15}O-water and ^{82}Rb (modified method).

^{82}Rb Versus ^{15}O-Water MBF

The global MBF values obtained from 14 subjects at rest and during stress using the modified ^{82}Rb method correlated better with those obtained using ^{15}O-water ($r = 0.92$) than with those obtained using the established method ($r = 0.60$), ($P < .01$) (Figure 2). Furthermore, the linear-regression slope was closer to unity with the modified method than with the established method (0.88 vs 0.44) indicating less bias ($P < .05$).

Inter-operator Repeatability of 3D ^{82}Rb MBF

Significantly improved inter-operator repeatability of regional MBF quantification (448 segments from fourteen subjects at rest and stress) was obtained using the modified method ($r = 0.89$, RPC%=4.7%) than with the established method ($r = 0.82$, RPC% = 5.6%) ($P < .01$) (Figure 3).

Regional Heterogeneity of 3D ^{82}Rb MBF

The previously established one-compartment model showed significant regional heterogeneity, with higher average ^{82}Rb MBF at rest in the septal region (1.62 ± 0.52 mL/minute/g) than in the lateral region (1.28 ± 0.47) ($P < .01$). The two-compartment model with wavelet-based noise reduction method also showed some regional heterogeneity, with higher average ^{82}Rb MBF at rest in the septal region (1.47 ± 0.61 mL/minute/g) than in the lateral region (1.21 ± 0.37) ($P < .01$). Our modified spillover correction method

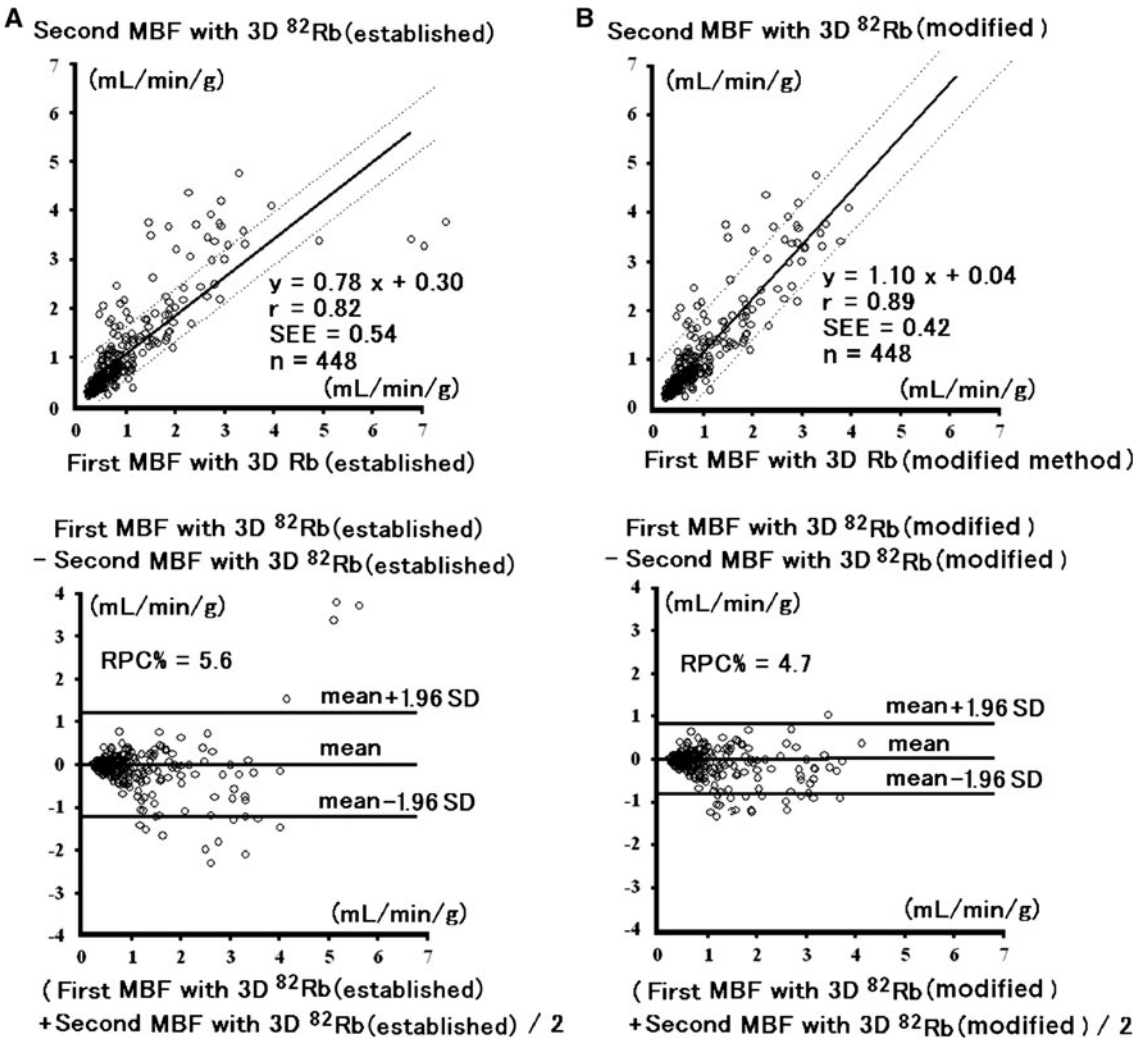

Figure 3. **A** Correlation and Bland-Altman plots of regional MBF test-retest repeatability with 3D ^{82}Rb (established method). **B** Correlation and Bland-Altman plots of regional MBF test-retest repeatability with 3D ^{82}Rb (modified method).

showed improved regional homogeneity, with no significant differences in MBF in these same regions (1.18 ± 0.41, 1.09 ± 0.35) (P = ns) (Figure 4).

Simulation Studies of Sensitivity to Error in PTF

Figure 5 shows the results of the simulation studies, which demonstrate the effect of error in the parameter PTF on MBF values for both the established and modified dual-spillover methods. Relatively less error was induced in MBF with the modified method. With the established method, an overestimation of 5% in PTF caused an overestimation of approximately 25% in MBF, while with the modified method the overestimation was suppressed to 10%. With the established method, an underestimation of 5% in PTF caused an underestimation of approximately 23% in MBF, while with the modified method the underestimation was suppressed to 15%.

Subjects with Known or Suspected CAD

The CAD patient demographics have been presented previously.[29] Briefly, the mean age of 12 consecutive patients was 70.8 ± 10.2 years (6 men). Nine patients had known CAD and 3 patients had suspected CAD. There was no significant difference in rest MBF determined using the established model versus the global input function model (Table 2). The hyperemic MBF was lower in stenotic segments ($P \leq .05$) than in non-stenotic segments as determined using the global input function model as well as the established model. Coronary flow reserve (CFR) was also reduced in the stenotic segments as determined using both models.

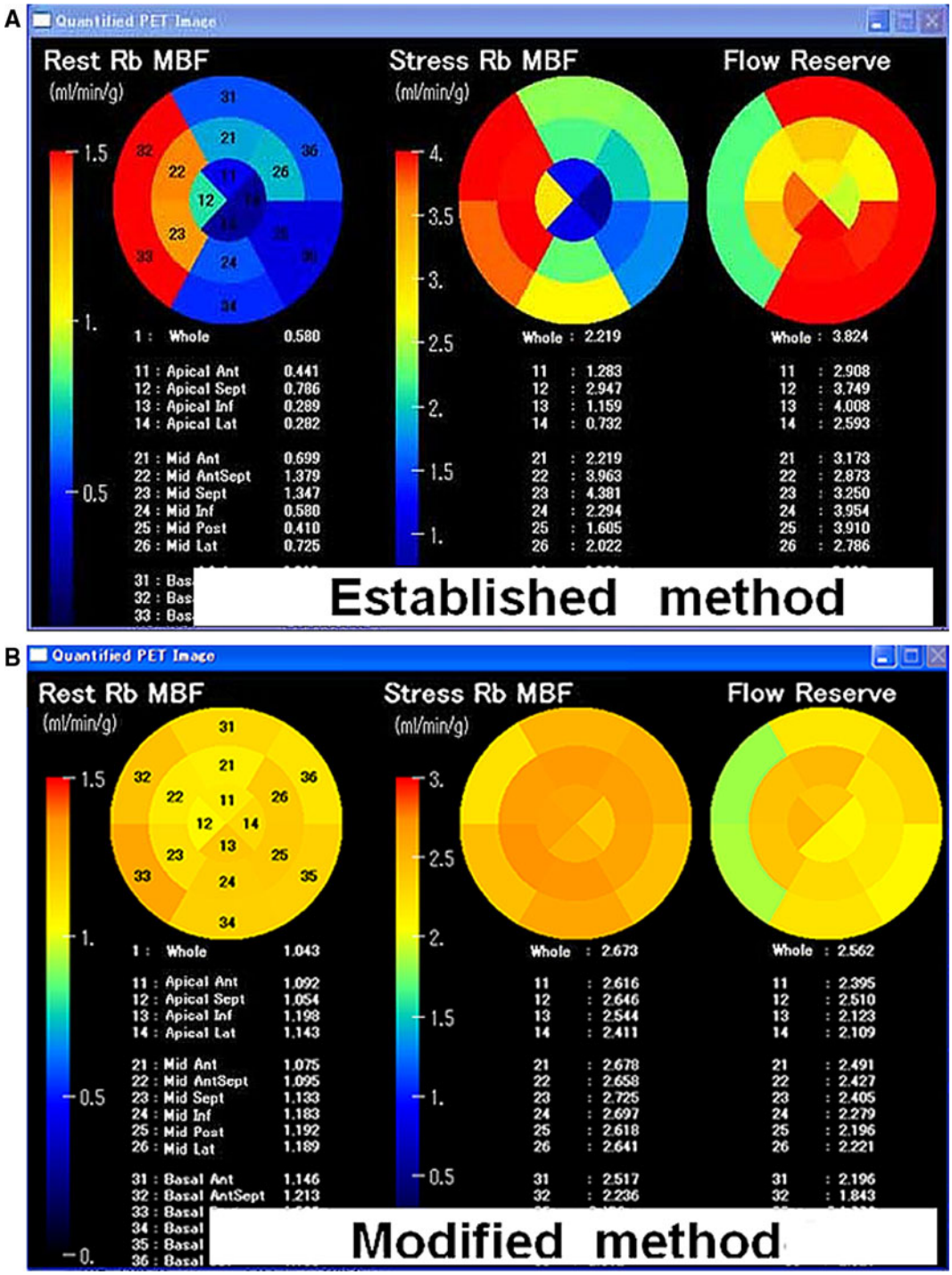

Figure 4. An example subject whose regional MBF in the septal region yielded higher estimates with the established method due to high spillover both from the right ventricle and from the left ventricle. The modified method with a uniform input function $Ca^{whole}(t)$ and with weighted fitting, estimated more homogeneous regional MBF due to appropriate correction of spillover from the blood into the myocardium.

DISCUSSION

^{82}Rb and 3D dynamic PET may allow for MBF quantification without a cyclotron.[5] However, it has been difficult to estimate MBF using 3D data acquisition with high repeatability.[29] In this study, we developed a modified method for MBF quantification with 3D ^{82}Rb

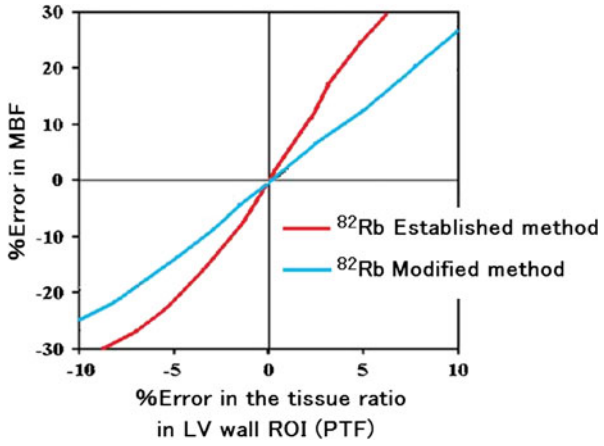

Figure 5. Simulations demonstrate the effect of error in the parameter PTF (tissue fraction in the myocardial wall ROI) ranging from −10% to +10%. Lower error in estimated MBF is observed with the modified method than with the conventional method.

using a dual-spillover model and blood-input-weighted fitting. Using this modified algorithm, 3D ^{82}Rb MBF correlated well and agreed with 2D ^{15}O-water MBF values. This method also demonstrated improved inter-operator repeatability over our previous established method,[2] partly due to improved stability in estimating regional MBF using ^{82}Rb.

3D ^{82}Rb MBF Measurements

Most of the current PET/CT scanners have only a 3D data-acquisition mode available. 3D mode acquisitions can reduce patient radiation exposure and can also prolong the generator's usable lifetime.[30] On the other hand, without septa in the 3D PET scanner, prompt-gammas, scatter, and the associated noise are increased, which may cause deterioration in image quality and may increase variability. Therefore, 2D data acquisition has been the standard approach for MBF quantification with ^{82}Rb.[1,5] Our group has performed 3D data acquisition previously for MBF quantification using ^{82}Rb. Hyperemic MBF is more variable than rest MBF,[2] which may be partially explained by reduced ^{82}Rb extraction at higher MBF.[21] The relatively long positron range and spillover from the LV and right ventricular (RV) cavities may also contribute to increased MBF variability with ^{82}Rb. In this study, we designed a software algorithm for defining a 3D ROI of the whole LV myocardium. A myocardium-to-blood pool spillover correction algorithm was implemented to reduce bias in the LV blood signal. Compared to the previous approach, rest and hyperemic MBF showed better correlation with that using 2D ^{15}O-water as the standard for comparison. Our modified method improved the repeatability coefficient; however, there was still relatively high variability using our modified approach. Inter-operator variability using other established PET myocardial perfusion tracers has been reported. Previous reports showed lower variability using O-15-labeled water (0.17 at rest and 0.43 mL/minute/g at stress).[31] N-13 ammonia PET MPI also showed less variability (0.20 at rest and 0.3 during cold pressor test).[32] The variability in this study was nearly 1 mL/minute/g with combined rest and stress MBF, which is higher than in previous reports. This larger variability may depend on the physical characteristics of ^{82}Rb, with a very short half-life, high-energy positron and 777 keV prompt gamma-ray.[33] These result in high prompt-gamma and Compton scatter components, especially using 3D PET acquisition compared to previous 2D PET studies using O-15 water and N-13 ammonia. Further technical improvement may be needed to overcome these physical characteristics of ^{82}Rb and to reduce the variability using ^{82}Rb and 3D PET.

A wavelet-based noise-reduction protocol can improve the signal-to-noise ratio of time-activity curves

Table 2. Regional MBF data in patients with CAD

	Stenotic region (n = 12)	Non-stenotic region (n = 24)	*P* value
Rest			
Global input function	0.93 ± 0.15	0.95 ± 0.17	n.s.
Established model[2]	0.91 ± 0.27	0.94 ± 0.36	n.s.
Stress			
Global input function	1.03 ± 0.28	2.80 ± 0.61	<.05
Established model[2]	1.13 ± 0.43	2.67 ± 1.06	<.05
CFR			
Global input function	1.24 ± 0.39	2.95 ± 0.55	<.05
Established model[2]	1.28 ± 0.44	2.87 ± 0.71	<.05

derived from dynamic PET images with ^{82}Rb.[4] The two-compartment model with wavelet-based noise reduction approach is an established method. This method has been validated only for 2D data acquisition, however, it could be expected to apply for 3D data acquisition as well.

Effect of the Uniform Input Function

For robust estimation of regional K1 and MBF, our modified method calculated regional $K1$ values using a uniform global input function $Ca^{whole}(t)$, which was estimated from a 3D ROI of the whole myocardium (Figure 1). The previously established method estimated the input function independently for each regional myocardial TAC, resulting in less stable MBF estimation. Increased stability with the modified method is likely due to less noise in the uniform pure blood curve. In addition, having fewer free parameters in the optimization function likely reduces the regional variability of parameters by improving numerical stability. We previously applied this global input function approach in ^{15}O-water PET and were able to detect reduced blood flow response in patients with CAD and Kawasaki disease.[17,26] In this study, our global input function model was able to detect reduced MBF in stenotic regions during pharmacological stress as well as the established model using 2D ^{82}Rb. Thus, we expect this global input function method using 3D ^{82}Rb should apply in patients with CAD. However, this approach requires further evaluation..

We designed an algorithm to set a 3D ROI of the whole myocardium and divide it into 16 segments automatically, thus removing some sources of variability in the process, which is also very time-consuming if performed manually. Currently, our ROI-setting software requires a few manual interactions, but it enables near operator-independent ROI definition and stable regional MBF quantification.

Sensitivity of MBF to Error in PTF

A simulation study (Figure 5) showed lower sensitivity of MBF quantification to the tissue fraction (PTF) in the LV wall ROI with the modified method than with the established method. MBF operator variability was also reduced with the modified method. Applying a weighted fitting and using a uniform input function $Ca^{whole}(t)$ might contribute to the reduction of error. The value $(1 - \beta)$ is the contribution ratio of the whole myocardial radioactivity and is an anatomical parameter for the whole LV myocardium. Thus, in the modified method, the parameter β was applied to the whole myocardial data.[28]

Effect of the Weighted Fitting

To improve the stability of measurements of regional K1 and MBF, the pure blood input curve $Ca^{whole}(t)$ was adopted as the weighting function in the nonlinear fitting analysis to suppress the spillover from the blood. Figure 4 showed that the established method overestimated the septal MBF due to spillover from the blood activity in both right and left ventricles. The modified method showed less bias from spillover in the septal region. The error weighted by the blood activity $Ca^{whole}(t)$ enforced strict tolerance in the curve-fitting during the timeframes of high radioactivity in the blood. The modified method enabled the suppression of spillover from the blood into the myocardium. Therefore, our modified method might have a better correlation in the repeated measurement values of regional MBF than did the established method. This result implies that our modified method may also be able to detect regional MBF reduction in patients with CAD.

Clinical Indications

PET MBF measurements represent a physiological approach using a bioactive tracer that is non-invasive and relatively simple to apply. In the past, these PET measurements have been performed using either ^{13}N-ammonia or ^{15}O-water with 2D PET imaging. However, ^{13}N-ammonia and ^{15}O-water require an on-site cyclotron. Thus, these approaches have not been widely available in the clinical routine. 3D PET scanners are being installed on an increasing basis, and there are more than 1000 PET or PET/CT scanners in North America and Europe to date[36] mainly for oncology imaging. In these centers, it would also be possible to perform MBF measurements using ^{82}Rb. ^{82}Rb has a very short physical half-life (76 seconds) and the generator can provide radiotracer doses at 6-minute intervals, allowing for repeat MBF measurements to be taken within a very short time span.[7] In the current protocol, rest and pharmacological stress measurements were completed in approximately 30 minutes. Thus, ^{82}Rb PET coronary vascular function tests can be applied to many patients in a clinical setting.[34]

Study Limitations

The principal difficulty in validating the new method was the lack of an ex vivo gold standard to determine the success of our algorithm. Therefore, we relied primarily on the MBF data from 2D ^{15}O-water PET using our program to improve the accuracy and reliability of ^{82}Rb MBF values with 3D data acquisition in comparison to the standard values.[28]

Our ROI-definition software requires few manual-handling steps; it enables almost operator-independent ROI definition thereby contributing to reproducible regional MBF quantification. Consequently, there was no significant difference in MBF results obtained by the expert user and the novice user. A novice operator was employed to verify the robustness of our ROI-setting program, which yielded operator-independent estimates. Intra-operator variability is expected to be less than inter-operator variability with our nearly operator-independent ROI-definition algorithm.[28]

In this study, we performed ^{82}Rb cardiac PET scans without correction of misalignment due to respiratory and cardiac motion between transmission and emission images. This misalignment can cause errors in quantification of MBF. Further validations with respiratory and electro cardiac gated imaging are needed.[35,36]

In this study, we acquired ^{82}Rb data using an HR+ PET scanner. Compared to images from current PET/CT scanners, the image quality may be slightly lower. However, the HR+ PET scanner can perform 2D and 3D data acquisitions. Head-to-head comparison is particularly important for this evaluation. Our new approach can be applied in current PET/CT scanners and might significantly enhance the ability to perform routine MBF quantification. This possibility requires further investigation.

CONCLUSION

We have developed a modified method for regional MBF estimation with 3D ^{82}Rb, which was well correlated with that using 2D ^{15}O-water, and demonstrated good inter-operator repeatability. The algorithm allows for simpler and more stable estimation of regional MBF using 3D ^{82}Rb PET, in comparison with previously established methods.

Acknowledgments

The authors thank Sayaka Takamori, RT; Keiichi Magota, RT; Hiroshi Arai, RT; Hidehiko Omote, RT; Kyotaro Suzuma, MS; and Ken-ichi Nishijima, PhD, for their technical expertise, and Eriko Suzuki for her administrative support of this study. This study was supported in part by grants from the Ministry of Education, Science and Culture (No. 19591395), Northern Advancement Center for Science & Technology (Sapporo, Japan) (Grant #H19-C-068, H23-S2-17), and Adult Cardiovascular Research Foundation (Kyoto Japan). Ran Klein was supported by the Japan Society for the Promotion of Science (JSPS) and Natural Sciences and Engineering Research Council of Canada (NSERC) Summer Program (2008) (Tokyo, Japan and Ottawa, Ontario, Canada).

APPENDIX

^{15}O-Water Model

The myocardium was modeled as a partial-volume mixture of arterial blood Ca(t) and tissue Ct(t) activity concentrations as in Eq. 1 (see below) where PTF denoted perfusable tissue fraction, VA is the fractional arterial blood volume, and ρ is the density of tissue (1.04 g/ml).

$$\mathrm{R}(t) = \mathrm{PTF} \cdot \rho \cdot \mathrm{Ct(t)} + \mathrm{VA} \cdot \mathrm{Ca(t)} \qquad (1)$$

The change in tissue activity concentration was modeled using the 1-tissue compartment model in Eq. 2 (see below) where F denotes blood flow in mL/minute/g. The parameter ρ is the partition coefficient of water in the myocardium and is equal to 0.91.

$$\mathrm{dCt}(t)/\mathrm{d}t = F \cdot \mathrm{Ca}(t) - (F/\rho) \cdot \mathrm{Ct}(t) \qquad (2)$$

In the LV blood cavity, activity concentration was modeled as a partial-volume mixture of $\beta = 85\%$ arterial blood and (1 - $\beta = 15\%$) myocardial tissue as shown in Eq. 3.

$$\mathrm{LV(t)} = \beta \cdot \mathrm{Ca(t)} + (1 - \beta) \cdot \rho \cdot \mathrm{Ct(t)} \qquad (3)$$

Equations 1, 2, and 3 were solved with a nonlinear least-squares analysis to estimate PTF, VA, and F, which was used as the estimate of MBF.

^{82}Rb Models

Established method. The measured tissue TAC in each myocardial ROI, R(t), during the entire scan length was estimated using Eq. 1. The change in tissue activity concentration was modeled using the one-tissue compartment model

$$\mathrm{dCt(t)/dt} = K1 \cdot \mathrm{Ca(t)} - k2 \cdot \mathrm{Ct(t)} \qquad (4)$$

where $K1$ (mL/minute/g) is the uptake rate from blood into the tissue and $k2$ (/minute) is the washout rate from myocardial tissue into the blood Ca(t) (Bq/mL). Radioactivity in the LV blood pool was calculated using Eq. 3 with $\beta = 85\%$.

The parameters PTF, VA, $K1$, and $k2$ were derived by nonlinear least-squares minimization using Eqs. 1, 3, and 4, where PTF represents the tissue fraction in the LV myocardium ROI.

Thus, the spillover-corrected pure blood Ca(t) for each segment was estimated. Conversion from $K1$ to MBF was estimated with the modified Renkin-Crone model[1,27] as shown in Eq. 5.

$$K1 = \mathrm{MBF}[1 - 0.86 \exp(-0.543/\mathrm{MBF})] \qquad (5)$$

Modified or dual-spillover method. Regional myocardial ROI data, R(t), were then analyzed using Eqs. 6 and 7.

$$\mathrm{R(t)} = \mathrm{PTF} \cdot \rho \cdot \mathrm{Ct(t)} + \mathrm{VA} \cdot \mathrm{Ca^{whole}(t)} \quad (6)$$

$$\mathrm{dCt(t)/\ dt} = K1 \cdot \mathrm{Ca^{whole}(t)} - k2 \cdot \mathrm{Ct(t)} \quad (7)$$

The regional myocardial ROI curve and left ventricular ROI blood curve (R(t) and LV(t), respectively) were sampled from the dynamic image as in the established conventional method and were assumed to be a linear combination of the uniform blood $\mathrm{Ca^{whole}}(t)$ and myocardium Ct(t) as in Eqs. 1 and 3. In addition, the relationship between $\mathrm{Ca^{whole}}(t)$ and Ct(t) was defined by the one-tissue-compartment model as in Eq. 7.

The parameters PTF, VA, $K1$, and $k2$ were simultaneously estimated by minimizing the weighted error (ε) as shown in Eq. 8 between the measured curve R(t) and the model in Eq. 6. The error was weighted by the blood activity concentration $\mathrm{Ca^{whole}}(t)$ to enforce strict tolerance in the curve fitting during the timeframes corresponding to high radioactivity in the blood.

$$\varepsilon = \Sigma[\mathrm{Ca^{whole}(t)} \cdot (\mathrm{PTF} \cdot \rho \cdot \mathrm{Ct(t)} + \mathrm{VA} \cdot \mathrm{Ca^{whole}(t)} - \mathrm{R(t)})]^2 \quad (8)$$

$K1$ values were converted into MBF using the Renkin-Crone extraction function as in Eq. 5.[3]

The estimated MBF values from the established uniform and modified weighted methods were compared against MBF values estimated from the corresponding ^{15}O-water images.

References

1. Manabe O, Yoshinaga K, Katoh C, Naya M, DeKemp RA, Tamaki N. Repeatability of rest and hyperemic myocardial blood flow measurements with 82Rb dynamic PET. J Nucl Med 2009;50:68-71.
2. Lortie M, Beanlands RS, Yoshinaga K, Klein R, Dasilva JN, DeKemp RA. Quantification of myocardial blood flow with 82Rb dynamic PET imaging. Eur J Nucl Med Mol Imaging 2007;34:1765-74.
3. Yoshinaga K, Manabe O, Katoh C, Chen L, Klein R, Naya M, et al. Quantitative analysis of coronary endothelial function with generator-produced 82Rb PET: Comparison with 15O-labelled water PET. Eur J Nucl Med Mol Imaging 2010;37:2233-41.
4. Lin JW, Sciacca RR, Chou RL, Laine AF, Bergmann SR. Quantification of myocardial perfusion in human subjects using 82Rb and wavelet-based noise reduction. J Nucl Med 2001;42:201-8.
5. El Fakhri G, Kardan A, Sitek A, Dorbala S, Abi-Hatem N, Lahoud Y, et al. Reproducibility and accuracy of quantitative myocardial blood flow assessment with (82)Rb PET: Comparison with (13)N-ammonia PET. J Nucl Med 2009;50:1062-71.
6. Yoshinaga K, Klein R, Tamaki N. Generator-produced rubidium-82 positron emission tomography myocardial perfusion imaging: From basic aspects to clinical applications. J Cardiol 2010;55:163-73.
7. Yoshinaga K, Chow BJ, deKemp RA, Thorn S, Ruddy TD, Davies RA, et al. Application of cardiac molecular imaging using positron emission tomography in evaluation of drug and therapeutics for cardiovascular disorders. Curr Pharm 2005;11:903-32.
8. Klein R, Beanlands RS, deKemp RA. Quantification of myocardial blood flow and flow reserve—technical aspects. J Nucl Cardiol 2010;17:555-70.
9. Slomka PJ, Le Meunier L, Hayes SW, Acampa W, Oba M, Haemer GG, et al. Comparison of myocardial perfusion 82Rb PET performed with CT- and transmission CT-based attenuation correction. J Nucl Med 2008;49:1992-8.
10. Bateman TM, Heller GV, McGhie AI, Friedman JD, Case JA, Bryngelson JR, et al. Diagnostic accuracy of rest/stress ECG-gated Rb-82 myocardial perfusion PET: Comparison with ECG-gated Tc-99m sestamibi SPECT. J Nucl Cardiol 2006;13:24-33.
11. Beanlands RS, Chow BJ, Dick A, Friedrich MG, Gulenchyn KY, Kiess M, et al. CCS/CAR/CANM/CNCS/CanSCMR joint position statement on advanced noninvasive cardiac imaging using positron emission tomography, magnetic resonance imaging and multidetector computed tomographic angiography in the diagnosis and evaluation of ischemic heart disease—executive summary. Can J Cardiol 2007;23:107-19.
12. Sampson UK, Dorbala S, Limaye A, Kwong R, Di Carli MF. Diagnostic accuracy of rubidium-82 myocardial perfusion imaging with hybrid positron emission tomography/computed tomography in the detection of coronary artery disease. J Am Coll Cardiol 2007;49:1052-8.
13. Lertsburapa K, Ahlberg AW, Bateman TM, Katten D, Volker L, Cullom SJ, et al. Independent and incremental prognostic value of left ventricular ejection fraction determined by stress gated rubidium 82 PET imaging in patients with known or suspected coronary artery disease. J Nucl Cardiol 2008;15:745-53.
14. Yoshinaga K, Chow BJ, Williams K, Chen L, deKemp RA, Garrard L, et al. What is the prognostic value of myocardial perfusion imaging using rubidium-82 positron emission tomography? J Am Coll Cardiol 2006;48:1029-39.
15. Bengel FM, Higuchi T, Javadi MS, Lautamaki R. Cardiac positron emission tomography. J Am Coll Cardiol 2009;54:1-15.
16. Yoshinaga K, Tamaki N, Ruddy T, DeKemp RA, Beanlands R. Evaluation of myocardial perfusion. Principles and practice of PET and PET/CT. 2nd ed., 2009Philadelphia, PA: Lippincott Williams and Wilkins; 2009. p. 541-64.
17. Yoshinaga K, Katoh C, Noriyasu K, Iwado Y, Furuyama H, Ito Y, et al. Reduction of coronary flow reserve in areas with and without ischemia on stress perfusion imaging in patients with coronary artery disease: A study using oxygen 15-labeled water PET. J Nucl Cardiol 2003;10:275-83.
18. Parkash R, deKemp RA, Ruddy TD, Kitsikis A, Hart R, Beauchesne L, et al. Potential utility of rubidium 82 PET quantification in patients with 3-vessel coronary artery disease. J Nucl Cardiol 2004;11:440-9.
19. Camici PG, Crea F. Coronary microvascular dysfunction. N Engl J Med 2007;356:830-40.
20. Klein R, Renaud JM, Ziadi MC, Thorn SL, Adler A, Beanlands RS, et al. Intra- and inter-operator repeatability of myocardial blood flow and myocardial flow reserve measurements using Rubidium-82 PET and a highly automated analysis program. J Nucl Cardiol 2010;17:600-16.
21. Lautamäki R, George RT, Kitagawa K, Higuchi T, Merrill J, Voicu C, et al. Rubidium-82 PET-CT for quantitative assessment of myocardial blood flow: Validation in a canine model of coronary artery stenosis. Eur J Nucl Med Mol Imaging 2009;36:576-86.
22. Schepis T, Gaemperli O, Treyer V, Valenta I, Burger C, Koepfli P, et al. Absolute quantification of myocardial blood flow with 13N-ammonia and 3-dimensional PET. J Nucl Med 2007;48:1783-9.

23. Diamond GA, Forrester JS. Analysis of probability as an aid in the clinical diagnosis of coronary-artery disease. N Engl J Med 1979;300:1350-8.
24. Naya M, Tsukamoto T, Morita K, Katoh C, Furumoto T, Fujii S, et al. Olmesartan, but not amlodipine, improves endothelium-dependent coronary dilation in hypertensive patients. J Am Coll Cardiol 2007;50:1144-9.
25. Siegrist PT, Gaemperli O, Koepfli P, Schepis T, Namdar M, Valenta I, et al. Repeatability of cold pressor test-induced flow increase assessed with H(2)(15)O and PET. J Nucl Med 2006;47:1420-6.
26. Furuyama H, Odagawa Y, Katoh C, Iwado Y, Yoshinaga K, Ito Y, et al. Assessment of coronary function in children with a history of Kawasaki disease using (15)O-water positron emission tomography. Circulation 2002;105:2878-84.
27. Herrero P, Markham J, Shelton ME, Bergmann SR. Implementation and evaluation of a two-compartment model for quantification of myocardial perfusion with rubidium-82 and positron emission tomography. Circ Res 1992;70:496-507.
28. Katoh C, Morita K, Shiga T, Kubo N, Nakada K, Tamaki N. Improvement of algorithm for quantification of regional myocardial blood flow using 15O-water with PET. J Nucl Med 2004;45:1908-16.
29. Yoshinaga K, Katoh C, Manabe O, Klein R, Naya M, Sakakibara M, et al. Incremental diagnostic value of regional myocardial blood flow quantification over relative perfusion imaging with generator-produced rubidium-82 PET. Circ J 2011;75:2628-34.
30. deKemp RA, Yoshinaga K, Beanlands RS. Will 3-dimensional PET-CT enable the routine quantification of myocardial blood flow? J Nucl Cardiol 2007;14:380-97.
31. Nesterov SV, Han C, Mäki M, Kajander S, Naum AG, Helenius H, et al. Myocardial perfusion quantitation with 15O-labelled water PET: High reproducibility of the new cardiac analysis software (Carimas). Eur J Nucl Med Mol Imaging 2009;36:1594-602.
32. Schindler TH, Zhang XL, Prior JO, Cadenas J, Dahlbom M, Sayre J, et al. Assessment of intra- and interobserver reproducibility of rest and cold pressor test-stimulated myocardial blood flow with (13)N-ammonia and PET. Eur J Nucl Med Mol Imaging 2007; 34:1178-88.
33. Esteves FP, Nye JA, Khan A, Folks RD, Halkar RK, Garcia EV, et al. Prompt-gamma compensation in Rb-82 myocardial perfusion 3D PET/CT. J Nucl Cardiol 2010;17:247-53.
34. Machac J, Bacharach SL, Bateman TM, Bax JJ, Beanlands R, Bengel F, et al. Positron emission tomography myocardial perfusion and glucose metabolism imaging. J Nucl Cardiol 2006;13: e121-51.
35. Alessio AM, Kinahan PE, Champley KM. Attenuation-emission alignment in cardiac PET/CT based on consistency conditions. Med Phys 2010;37:1191-200.
36. Hunt DC, Easton H, Caldwell CB. Design and construction of a quality control phantom for SPECT and PET imaging. Med Phys 2009;36:5404-11.